Control of Feedback in Hearing Aids

B. Rafaely, M. Roccasalva-Firenze and E. Payne

ISVR Technical Memorandum 836

March 1999

SCIENTIFIC PUBLICATIONS BY THE ISVR

Technical Reports are published to promote timely dissemination of research results by ISVR personnel. This medium permits more detailed presentation than is usually acceptable for scientific journals. Responsibility for both the content and any opinions expressed rests entirely with the author(s).

Technical Memoranda are produced to enable the early or preliminary release of information by ISVR personnel where such release is deemed to the appropriate. Information contained in these memoranda may be incomplete, or form part of a continuing programme; this should be borne in mind when using or quoting from these documents.

Contract Reports are produced to record the results of scientific work carried out for sponsors, under contract. The ISVR treats these reports as confidential to sponsors and does not make them available for general circulation. Individual sponsors may, however, authorize subsequent release of the material.

UNIVERSITY OF SOUTHAMPTON

INSTITUTE OF SOUND AND VIBRATION RESEARCH

SIGNAL PROCESSING & CONTROL GROUP

Control of Feedback in Hearing Aids

by

B Rafaely, M Roccasalva-Firenze and E Payne

ISVR Technical Memorandum No. 836

March 1999

Authorised for issue by
Prof J K Hammond
Director

Control of Feedback in Hearing Aids

B Rafaely, M Roccasalva-Firenze and E Payne

Institute of Sound and Vibration Research, University of Southampton, UK

This report is presented as a series of two papers, describing the study into the feedback path variability in hearing aids, and a development of a new method to design hearing aid filters which provide the required compensation while ensuring robust stability thus preventing the "howling" due to feedback.

Feedback path variability in hearing aids

M. Roccasalva Firenze, B. Rafaely and E. Payne

Institute of Sound and Vibration Research, University of Southampton,

Southampton, SO17 1BJ, UK

Abbreviated title: Feedback in hearing aids

Corresponding author:

Boaz Rafaely

Institute of Sound and Vibration Research

University of Southampton,

Southampton, SO17 1BJ

UK

Email: br@isvr.soton.ac.uk

Tel: +44 (0)1703 593043

Fax: +44 (0)1703 593190

Abstract

Acoustic feedback is a common problem in vented hearing aids. Hearing aids designed to work under normal conditions, could go unstable when the feedback path varies under changing conditions. A comprehensive study of the variability of the feedback path under various conditions and for different users is presented in this paper. A multiplicative uncertainty bound is then suggested to model the variations, which is then used to formulate a condition on the stability of the hearing aid. Examples of robust constant amplification hearing aids are presented. The robust stability condition is then suggested as a tool to design more robust hearing aids.

PACS number: 43.66.Ts, 43.66.Yw

Introduction

Acoustic feedback is a severe problem in hearing aids. The feedback occurs when the receiver of the aid produces an acoustic signal that leaks back to the microphone, causing instability and oscillations leading to a high frequency whistling sound produced by the hearing aid. Reducing the hearing aid gain reduces the feedback signal, but also degrades the hearing aid performance. In most cases the vent is the principle cause of the acoustic feedback in the hearing aids. Venting, however, is necessary to provide a more natural sound by reducing the occlusion effect which hearing aid users often experience when venting is insufficient.[1] The feedback problem is worse for in-the-ear and in-the-canal hearing aids due to the shorter distance between the microphone and the vent opening, and the increased coupling between the receiver and the microphone.

Various approaches have been reported which attempt to reduce the feedback problem. Low pass filtering was used to roll off the high frequency response of the hearing aid, thus reducing the level of the high frequency feedback signals, but this can detrimentally attenuate the high frequency gain of the hearing aid.[2] An alternative method is phase cancellation where the effect of acoustic feedback can be reduced by altering either the magnitude or the phase of the hearing aid feedback-loop[3]. More complex methods for feedback suppression involve various techniques of digital signal processing[4,5], where adaptive filters are used to generate an estimate of the feedback signal and subtract it from the feedback signal measured by the microphone, thus reducing its effect. Variations of this method with different implementations of the adaptive filter are reported in recent studies [6-10].

Although many of the adaptive feedback cancellation systems are useful in reducing the feedback problem to a limited extent, the feedback path model used is never perfect, due to both modelling errors and time-variability of the feedback path. To maintain stability, the hearing aid system must therefore be *robust* to any variations or uncertainty in the feedback path[11], which are not accounted for by an adaptive feedback cancellation filter.

The aim of this paper is to study the feedback path and its variability between users and under various conditions. This data could then be used in designing more robust hearing aids. Changes in the feedback path may be caused by many factors. Movements of the head and mouth can alter the hearing aid fitting and the amount of sound that leaks to the microphone. The acoustic characteristic of the ear, which depend on the ear canal shape and the eardrum impedance, varies between subjects and ears, and can affect the pressure generated by the receiver in the ear. Changes in the feedback path can also occur if the microphone of the hearing aid is covered, for example, by the positioning of a telephone receiver near the ear.

The main contribution of this paper is the comprehensive analysis of the variability of the feedback path in hearing aids, and the formulation of robust stability conditions from the bounds on the feedback path variability, which can be used in the design of robust hearing aid filters.

The paper is organised as follows. Section I describes the hearing aid system used here, and in section II the feedback problem is described from a control view point. Sections III, IV and V present measurements of the feedback path in real ears, analysis of the feedback path uncertainty and discussion of the results, respectively.

I. The hearing aid system

An in-the-ear hearing aid as used in this study is shown in Figure 1. The principal components of the system are the microphone, the hearing aid circuit (amplifier), the receiver and the vent. The external sound is detected by the microphone, amplified by the hearing aids circuit and transmitted into the ear canal by the receiver. The vent connects the ear canal to the outside, and transmits back the sound from the ear canal to the microphone causing the feedback problem. The hearing aid feedback mechanism is well explained in previous works[12,13], and is illustrated by the block diagram in Figure 2, where P_{ext} is the sound pressure outside the ear, P_{ear} is the sound pressure in the ear canal, A is the transfer function of the unamplified signal path directly through the vent into the ear canal, B is the transfer function of the acoustic feedback path from the ear canal through the vent, M is the electroacoustic transfer function of the microphone, R is the electroacoustic transfer function of receiver and H is the transfer function of the hearing aid circuit and in this study it represents a constant gain.

The open-loop acoustic gain is defined in the frequency domain as:

$$F = MHR \qquad (1)$$

and the open-loop gain with unity amplification, $H=1$, is defined as:

$$F_0 = MR \tag{2}$$

The acoustical feedback path is defined as:

$$G = RBM \tag{3}$$

and the complete acoustic transfer function of the system is now written using Figure 2 as:

$$\frac{P_{ear}}{P_{ext}} = A + \frac{MHR}{1 - MHRB} = A + \frac{F}{1 - GH} = A + \frac{F_0 H}{1 - GH} \tag{4}$$

A Starkey's In-The-Ear hearing aid (ITE 11M) was used in this study with the microphone and the receiver of the hearing aid disconnected from the hearing aid circuit to allow external measurement. An experiment was designed to study the various elements of this hearing aid system, as illustrated in Figure 2, which were then used below to simulate the hearing aid response in various conditions. To achieve accurate simulation, the contribution of the various blocks in Figure 2 had to be studied carefully. In this experiment the hearing aid was attached to a vented earmould and placed in a 2-branch occluded ear simulator, Industrial Research Products Inc. model XD1053, with a Brüel & Kjær (B&K) microphone (4165) placed at the eardrum position. Another B&K microphone was placed externally to measure the external pressure. The complete system was placed in an B&K anechoic chamber (4222), as illustrated in Figure 3.

A. Feedback path G

The frequency response of the feedback path (G) between the receiver input and the microphone output with the amplifier H disconnected was measured using an Adavantest FFT servo analyser (R9211B/C), and is shown in Figure 4. The high frequency peaks are mainly due to the receiver response.

B. Unamplified acoustic path A

The acoustical response from the external pressure to the pressure in the ear canal with the amplifier H disconnected, denoted by A in Figure 2 was obtained by measuring the frequency response between the internal B&K microphone and the external B&K microphone. Figure 5 shows the measured frequency response of path A, where two resonance peaks at 378 Hz and at 9.2 kHz are observed. The low frequency resonance is due to the vent inertia and the ear canal compliance, while the high frequency resonance is due to standing waves in the vent.

C. Amplified signal path

The complete amplified path, as defined in equation (4) includes both the acoustic path A, which was measured separately above, and the electronically amplified path F defined in equation (1). To measure F accurately, the vent was blocked so that the contribution of the acoustic path A was significantly reduced. However, the acoustic impedance of the ear canal is dependent on the vent, specially at low frequencies, so the measured response F had to be corrected to simulate an open vent. This correction was found by comparing the pressure at the ear canal produced by the receiver, for

open and blocked vents. Figure 6 shows the amplified response F_o, for a unity gain ($H=1$), as measured after correction. The complete amplified path P_{ear}/P_{ext}, as in equation (4), was measured with various gain values, $H = 20$, 30 and 40dB, using the experimental set-up as in Figure 3. The corresponding frequency response functions were then reconstructed using the separate measurements of A, G, F_0 and H as in equation (4). The comparison of the measured frequency response curves with the simulated curves, shown in Figure 7, illustrates that a good modelling of the various system paths was achieved. The modelled responses are used below in the stability and performance analysis of the hearing aid system.

II. The feedback path

Feedback occurs when a fraction of the receiver signal is transmitted back to the microphone, through the acoustic path (B) as in Figure 2. Acoustic feedback in hearing aids has been given many names in the literature such as howling, whistling, ringing or simply feedback. The acoustic path is the most significant contributor to the feedback signal, although electrical and mechanical paths also exist. In this study only the acoustical component is considered.

An electrical block diagram of the feedback part in the hearing aid system is illustrated in Figure 8, where H is the feedback path and H is the amplifier gain. The open-loop transfer function is defined as $L = -GH$ with the minus sign resulting from the positive summation of the feedback signal. The system of Figure 8 is stable according to the Nyquist criterion[14] if the Nyquist plot of $L(j\omega)$ encircle the (-1, $j0$) point as many times as there are right-half plane poles in $L(s)$, with the encirclement

made in the clockwise direction. If the open loop system $L(s)$ is stable, as in the case of the hearing aid system, the closed loop system will be stable if the Nyquist plot of $L(j\omega)$ does not encircle the critical $(-1, j0)$ point at all.[14]

Instability usually rises when a frequency component of the feedback signal arrives at the microphone in phase with the external signal component, but with greater magnitude. Then oscillation will occur, driving the hearing aid to its maximum level and rendering it useless. Previous studies[5] suggested that a gain margin of approximately 5dB from the instability point, might be sufficient to stop the howling in normal use. The frequency response and stability of the hearing aids used in this study were analysed for various gain level, H=20, 30, 40 and 47 dB. Figure 9 shows the simulated response of the hearing aid, as in equation (4), for the various gain values, and Figure 10 shows the corresponding Nyquist plots. It is shown that a gain of 47dB brings the system very close to instability, where the "whistling" is likely to occur around 5kHz. In fact, the system will go unstable if the constant gain is increased to 47.46dB. For the lower gain values, the amplification of the hearing aid is reduced, but stability margins are increased as expected.

III. Experimental evaluation of the Feedback path variability

The feedback path of a vented hearing aid play a dominant role in the feedback problems encountered by hearing aid users. A knowledge of the feedback path and its variability in real ears will assist in the design of hearing aids that are more robust and suffer less from the feedback problem. The acoustical feedback path G in human ears

can change for different subjects, ears and conditions. The causes of these changes are outlined below.

a)   Increase in the sound leaking from the ear to the outside. The movements of the head and of the mouth when smiling, laughing or eating and other conditions causing changes in the hearing aid fit, can change the level of the sound that leaks to the microphone.

b)   Change in the sound pressure level inside the ear canal. The acoustic characteristics of each ear, determined by the ear canal dimensions and eardrum impedance are unique, so the sound pressure developed inside the ear in response to the same receiver input will vary between ears.

c)   Change in the level of the feedback signal transmitted from the vent to the microphone. A hand or a phone handset covering the ear can increase the level of the feedback signal detected by the microphone.

An experiment was conducted to analyse the variability of the feedback path in various conditions that cause the changes described above. Eight conditions were chosen, as described below.

1. First normal fitting.

2. Second normal fitting. The ear mould and hearing aid were removed from the ear and refitted.

3. Hand positioned very close to the ear.

4. Hand positioned 10 cm from the ear.

5. Hand positioned 20 cm from the ear.

6. Open mouth.

7. Smiling face.

8. A wrong fitting, with the top prong of the ear mould not fitted correctly.

The experiment was conducted on six otologically normal subjects. The same hearing aid utilised in the first part of this study was used for this experiment. The measurements were conducted inside an Anechoic Chamber, and were performed using an FFT servo analyser. The receiver was driven by a multiple sine signal, in the range 300 Hz - 10,000 Hz of amplitude 0.2V. This amplitude was chosen to ensure that the noise level inside the ear canal was lower then 91dBA, to avoid any physical damage to the ear.[15] The sound travelling through the vent was detected by the microphone, and amplified by a low-noise pre-amplifier appropriately built for that microphone (Knowles EM3046), to enable detection of the low level feedback signal.

Figure 11 shows the various frequency response curves of the feedback path G in the nominal fit (condition 1), as measured in this experiment for the left and right ears of all six subjects. From 300Hz to about 1kHz the difference between the various curves is about 20dB, after which the difference increases to a value of about 50dB near 5kHz. Figures 12, 13 and 14 show the frequency response curves of G with the hearing aid fitted to one subject, under the different measurement conditions. In the measurements with a hand near the ear (Figure 12, conditions 3-5), it is evident that only when the hand is very close to the ear, the variation from the normal response (the first fitting) is large, particularly under 1kHz, where there is about 20dB difference. Above 1kHz, the effect of a hand near the ear seams to be smaller.

Figure 13 shows the measurement of the feedback path with an open mouth and smiling face (conditions 6 and 7), which where found to be very similar to the measurement with the normal fit, i.e. movement of the face and mouth were found to have little effect on the feedback path. The measurements with wrong fitting and a second normal fitting (conditions 2 and 8) are shown in Figure 14. Very small differences to the first normal fit were found below 2.8 kHz, while above 2.8 kHz the amplitude of the curve corresponding to the wrong fit varied up to 10dB from the normal fit.

Most conditions seem to have small effect on the feedback path, except the condition with a hand very close to the ear, and to some extent a wrong fitting, which had a more significant effect. Variability among subjects, also produced significant changes in the feedback path.

IV. Analysis of uncertainty

The variation of the feedback path for the measured data was analysed at four discrete frequencies, i.e. 0.5, 1, 3 and 5kHz. The complex values of the frequency response functions at these frequencies were plotted using a Nyquist plot, to evaluate the "spread" of the response in the various conditions. Two sets of measurement were defined and analysed separately. The first included the complete measurement set with all ears at all conditions. The second set included data from individuals ears in all conditions, taking into account that hearing aids are customised to individual subjects, thus excluding any inter-subject variability.

Figure 15 show the Nyquist plots for the first set with all subjects under all conditions. The figure shows the Nyquist plot of the feedback path of one ear under normal conditions at the full frequency range (solid curve), and the complex values of the feedback path of all ears under all conditions at the selected frequency only, marked by 'x'. The figure also shows a circle that forms a bound around all complex values, which is used in the next section for robust stability analysis. At lower frequencies, 500Hz and 1000Hz, most values are clustered together, while few values spread far from the rest. These extreme values are due to the more extreme conditions of placing a hand very close to the ear or wrong hearing aid fitting, which generate large low frequency variations. At higher frequencies, 3kHz and 5kHz, the variations are spread more evenly, which suggest that these variations occur more randomly between subjects. Figure 16 show the feedback path variations at the same discrete frequencies but for an individual ear, where only the measurements with that ear under all conditions were included. Note that the figures are scaled for better illustrate the various complex values at the selected frequencies. It can be seen that here, as well, at low frequencies the values are clustered closer together except the extreme cases, while at high frequencies they are spread more evenly in the complex plane.

From the analysis of these measurement sets, it is evident that the spread of the values in the complex plane form more clustered shapes that fill only small part of the circular bound due to the significant amplitude variations in the extreme cases at low frequencies, while at higher frequencies the spread is more even and the various values fill the circular bound more evenly. This analysis is used below in modelling the uncertainty of the feedback path to assist robust design of hearing aids.

V. Robust hearing aids

The knowledge of the uncertainty of the feedback path can be useful in designing a robustly stable hearing aids that maintain stability even when the response of the path changes. One way to describe variations or uncertainty, which is widely used in feedback control, is by a multiplicative uncertainty around a nominal model[11]. If G_0 is the nominal response of the feedback path, i.e. the response with normal fit, and $\tilde{G}$ is a set of measured feedback path response functions, than any response G from the set $\tilde{G}$, can be written in terms of the nominal response as:

$$G(j\omega) = G_0(j\omega)(1 + \Delta(j\omega))$$

(5)

where $\Delta(j\omega)$ can take any complex value, and is a function of frequency. $\Delta(j\omega)$ can be written as:

$$\Delta(jw) = \frac{G(jw)}{G_0(jw)} - 1$$

(6)

and its maximum value at any frequency for the complete set $\tilde{G}$, denoted by $W(\omega)$ is given by

$$W(w) = \max_{G \in \tilde{G}} |\Delta| = \max_{G \in \tilde{G}} \left| \frac{G(jw)}{G_0(jw)} - 1 \right|$$

(7)

Considering the Nyquist plot of the open-loop system $-GH$ as shown in Figure 17, the system with responses described by the multiplicative uncertainty bound $W(\omega)$, are represented as being inside a circle of radius $|WG_0H|$ around the nominal value $-G_0H$.

This uncertainty model fits reasonably well the variations of the feedback path presented above, specially at high frequencies, as discussed in section IV. It is next shown how the multiplicative uncertainty bound is related to the system stability, and what these bounds are for the hearing aid studied here. The hearing aid system, as shown in Figure 8, will be robustly stable, i.e. stable for all given variations in the feedback path, as long as the circle of uncertainty does not encircle the $(-1,j0)$ point for all ω. This follows directly from the Nyquist stability criterion discussed above. If

$$L_0 = -G_0 H \tag{8}$$

is the open loop response for the nominal feedback path G_0, and the distance between the circle centre and the $(-1,j0)$ point is $|1+L_0(j\omega)|$, than to maintain stability the circle radius must be smaller than that distance. The condition for robust stability is therefore written as[11]:

$$|W(\omega)L_0(j\omega)| < |1 + L_0(j\omega)| \quad \Rightarrow \quad \frac{|W(\omega)L_0(j\omega)|}{|1 + L_0(j\omega)|} < 1 \quad \text{for all } \omega \tag{9}$$

which can be written as

$$|W(\omega)T_0(j\omega)| < 1 \quad \text{for all } \omega \tag{10}$$

where T_0 is the nominal complementary sensitivity function given by $L_0/(1+L_0)$. The condition for robust stability given by equation (9) means that the hearing aid system with gain H and nominal feedback path G_0 will maintain stability for any variation of the feedback path from G_0, as long as this variation is bounded by W, and equation (9) is maintained.

Figure 18 shows the multiplicative uncertainty bound W calculated using equation (7) for the measurement set that included all data (upper curve), and for the measurement sets that included data from individual ears (lower curves). With all data included, the multiplicative uncertainty bound showed high values at lower frequencies due to the extreme cases, and at high frequencies due to the inter-subject variability and other conditions. The response with a normal hearing aid fitting in one specific subject was used as the nominal response G_0 in this case. With data from individual ears, the multiplicative uncertainty bound changes significantly between subject, due to the inter subject variability, and is also characterised by high values at both the low and high frequency bands. The response with normal hearing aid fitting of each individual ear was used as the nominal response G_0 in this case.

The uncertainty bounds calculated above were used in the design of the constant gain hearing aid used in this study. The maximum gain H was chosen such that the robust stability condition in equation (9) was still satisfied. Figure 19 shows the simulated hearing aid response, calculated using equation (3), under two different robust stability conditions, as shown in Figure 18. The first included the multiplicative uncertainty bound with all measured data, and the second included data from one individual subject. Also shown in Figure 19 is the hearing aid response with a gain of 47dB which brought the system close to instability. The figure show that with a gain of 36.9dB, the hearing aid was robust to variations in the feedback path of an individual subject, while with a gain of 21.9dB it was robust to inter-subject variability as well. This result indicate that a constant amplification hearing aid

designed to be robust to all users under all conditions will perform poorly, while a hearing designed for a given user will perform better, as expected. It should be noted that the computed uncertainty bounds where different for different ears, as illustrated in Figure 18. Therefore, the hearing aid gain has to be adjusted to each ear to achieve robust stability. This suggests that a customised hearing aid designed to be robustly stable will probably work better if the uncertainty of each custom ear could be obtained.

Figure 20 shows the quantity $|WT_0|$ which determines the robust stability condition as presented in equation (9) for the two constant amplification hearing aid systems designed above, showing that both systems do indeed maintain the robust stability condition. The condition is only active, however, over a narrow frequency band. A further analysis presented in Figure 21, where $|1/T_0|$ is compared to $W(\omega)$ for the two hearing aid systems. In this case the robust stability condition is written as $W(\omega)<|1/T_0|$. In both cases, any further increase in the hearing aid gain will violate the robust stability constraint at a narrow frequency band.

The results of Figure 20 and Figure 21 suggest that a higher order filter within the hearing aid circuit, such as a digital filter, designed to maintain the constraint more tightly over a wider frequency band by allowing different gains at different frequencies, could produce better performance without compromising robust stability. The use of the robust stability condition as presented here in the design of digital hearing aids is studied in a continuation work.

Conclusion

The variability of the feedback path in hearing aids was studied in this paper. An experiment was conducted to measure the variability of the feedback path for different subjects under various conditions. It was shown that the variations can be modelled reasonably well using a multiplicative uncertainty bound, widely used in robust control. A robust stability condition for the hearing aid system which is a function of the uncertainty bound was then formulated. Constant amplification hearing aids were then designed for maximum gain while maintaining robust stability under various conditions, showing clearly the trade-off between performance and robustness. The robust hearing aids design can be extended to digital hearing aids, where best compensation and robust stability are achieved simultaneously. This is further studied in a continuation work.

Acknowledgement

References

[1] The Earmould current practice and technology, Hearing Aid Audiology Group, British Society of Audiology, 1984.

[2] D.A. Preves, J.A. Sigelman, P.R. LeMay, A feedback stabilizing circuit for hearing aids, Hearing Instruments 37(4), 35-36, 1986.

[3] J.R. Wang, R. Harjani, Acoustic cancellation in hearing aids, Proceedings of the IEEE International Conference on Acoustics, Speech and Signal Processing, 137-140, 1993 .

[4] D.P. Egolf, Review of the Acoustic Feedback Literature from a Control System Point of View, The Vanderbilt Hearing-Aid Report, Edited by G.A. Studebaker and F.H. Bess, Monographs in Contemporary Audiology, 1982.

[5] N. Bisgaard, O. Dyrlund, Acoustic Feedback: Traditional feedback suppression methods, Hearing Instruments 42(9), 24-26, 1991.

[6] H.A.L. Joson, F. Asano, Y. Suzuki, and T. Sone, Adaptive feedback cancellation with frequency compression for hearing aids, J. Acoust. Soc. Am. 94 (6), 3248-3254, 1993.

[7] M.G. Siqueira, R. Speece, V. Petsalis, A. Alwan S. Soli and G. Gao, Subband adaptive filtering applied to acoustic feedback reduction in Hearing aids, Proceeding of the IEEE Asilomar Conference on Signal System, and Computer, November, 1996.

[8] S. Wyrsch, A. Kaelin, A DSP implementation of a digital hearing aid with recruitment of loudness compensation and acoustic echo cancellation, Workshop on application of signal processing to audio and acoustic, New Paltz, New York, 19-22 October, 1997.

[9] J.M. Kates, Feedback cancellation in Hearing Aids: Results from a computer simulation, IEEE Transaction on Signal Processing, 39(3), 553-562, March 1991.

[10] J.A. Maxwell, P.M. Zurek, Reducing Acoustic Feedback in Hearing Aids, IEEE Transaction on Speech and Audio Processing, 3(4), 304-313, July 1995.

[11] S. Skogestad, I. Postlethwaite, Multivariable Feedback Control, John Wiley & Sons, 1996.

[12] J.M. Kates, A computer simulation of hearing aid response and the effects of ear canal size, J. Acoust. Soc. Am. 83(5), 1952-1963, May 1988.

[13] D.P. Egolf, H.C. Howell, K.A. Weaver and D.S. Barker, The hearing aid feedback path: Mathematical simulations and experimental verification, J. Acoust. Soc. Am. 78 (5), 1578-1587, 1985.

[14] B.C. Kuo , Automatic Control system, Prentice Hall VII Edition 1995.

[15] Guide to Experimentation involving Human Subjects, ISVR Technical Memorandum No. 808, October 1996.

Figure captions

Figure 1 The hearing aid system.

Figure 2 A system block diagram for a vented hearing aid.

Figure 3 The experimental set-up in the anechoic chamber.

Figure 4 The measured frequency response of the feedback path G.

Figure 5 The measured frequency response of the unamplified signal path A.

Figure 6 The measured frequency response of the open loop with unity gain F_0.

Figure 7 A comparison between the measured frequency response curves (solid lines) and the simulated frequency response curves (dashed lines) for amplifier gain values of $H = 20\text{dB}$ (lower curves), 30dB (middle curves) and 40 dB (upper curves).

Figure 8 Electrical block diagram of the hearing aid as a feedback system.

Figure 9 Simulated hearing aid response curves using equation (4), with various gain values of $H = 20, 30, 40$ and 47 dB, as shown above.

Figure 10 Nyquist plot of ($-GH$) with various gains of $H = 20, 30, 40$ and 47 dB. The term $-GH$ is used rather than $+GH$ to account for the positive feedback defined in Figure 9.

Figure 11 Nominal response curves of the feedback path G for the left and right ears of all six subjects (condition 1).

Figure 12 Frequency response curves of the feedback path of one ear in different conditions of measurement: first normal fitting (condition 1, solid line), hand positioned very close to the ear (condition 3, dashed line), hand positioned 10 cm from the ear (condition 4, dotted line) and hand positioned 20 cm from the ear (condition 5, dash-dotted line).

Figure 13 Frequency response curves of the feedback path of one ear in different conditions of measurement: first normal fitting (condition 1, solid line), open mouth (condition 6, dashed line) and smiling face (condition 7, dash-dotted line).

Figure 14 Frequency response curves of the feedback path of one ear in different conditions of measurement: first normal fitting (condition 1, solid line), second

normal fitting (condition 2, dashed line) and wrong fitting (condition 8, dash-dotted line).

Figure 15 Nyquist plot of the feedback path variability which include all subjects under all conditions at several discrete frequencies, as shown above. The response in one ear under normal conditions is presented at the full frequency range (solid curve), while all other complex response values marked by 'x' are presented at the four discrete frequencies. A circle enclosing all response values is also presented.

Figure 16 Nyquist plot of the feedback path variability which include one ear under all conditions at several discrete frequencies as shown above. The response for that ear under normal conditions is presented at the full frequency range (solid curve), while all other complex response values marked by 'x' are presented at the four discrete frequencies. A circle enclosing all response values is also presented.

Figure 17 Nyquist plot of the open loop system $(-GH)$, showing the multiplicative uncertainty bound W as a circle around the nominal value.

Figure 18 The multiplicative uncertainty bound W for the measurement set with all subjects under all conditions (upper curve), and the multiplicative uncertainty bound W for individual ears under all conditions (lower curve).

Figure 19 Simulated hearing aid response curves calculated using equation (4) under two different robust stability condition as in equation (8). From top to bottom: close to instability with hearing aid gain of 47dB, robust stability for all subjects and conditions with a gain of 36.9dB, and robust stability for an individual ear variations with a gain of 21.9dB.

Figure 20 The robust stability condition $|WT_0|$ for the two hearing aids shown in Figure 19, with the 21.9dB gain (solid line) and 36.9dB gain (dashed line). Robust stability is maintained in both cases.

Figure 21 The robust stability bound W (dashed line) compared to $|1/T_0|$ (solid line) such that the robust stability condition becomes $W<|1/T|$, for the hearing aid design with the 21.9dB gain (upper curves; variation of all subjects and conditions) and 36.9dB gain (lower curves; variation for an individual ear). Robust stability is maintained exactly at a single frequency, and with large margins at other frequencies.

Figure 1
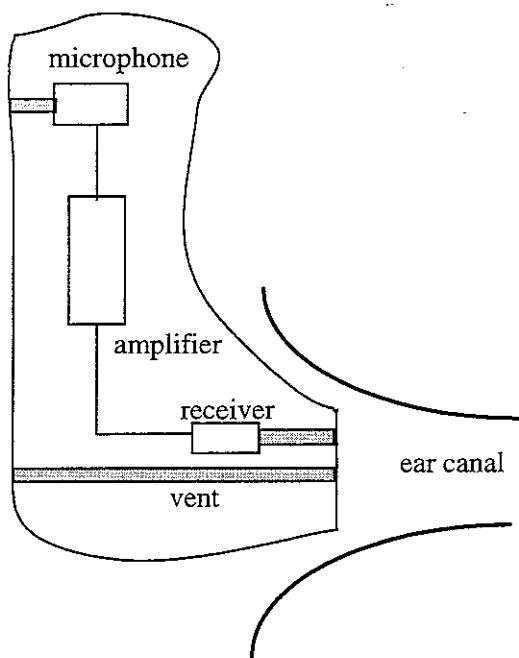
Figure 2
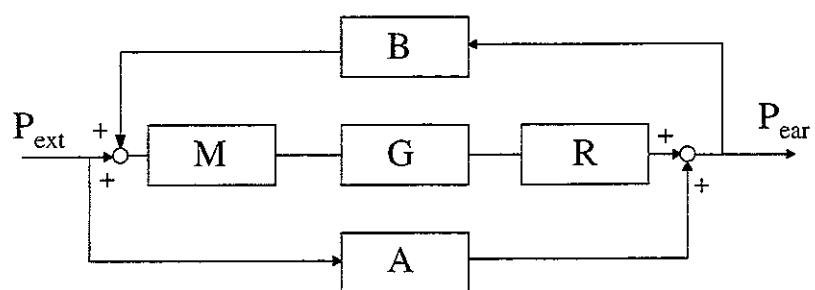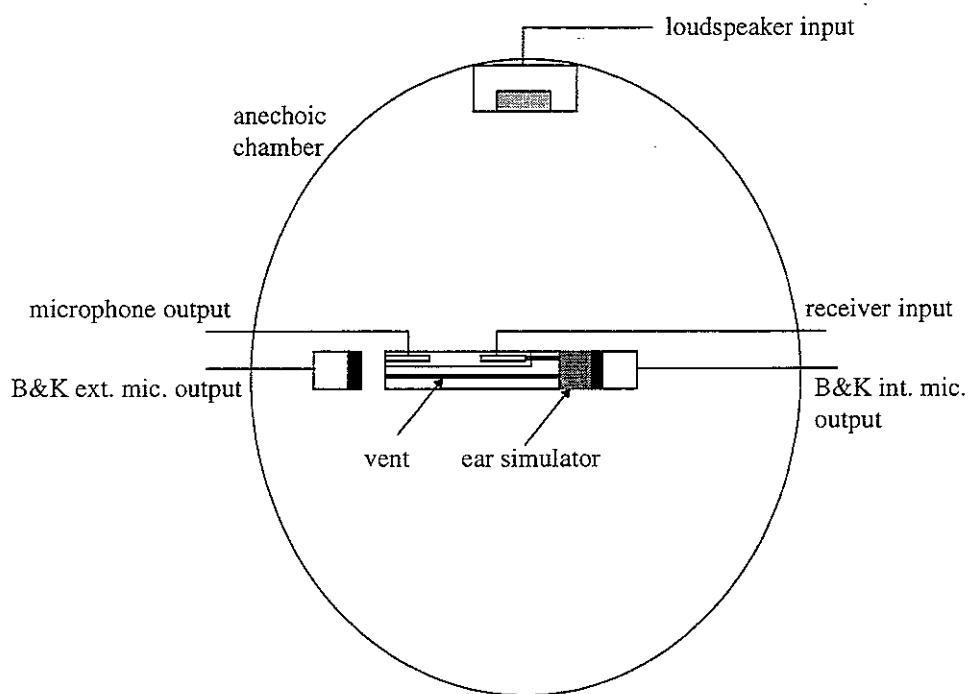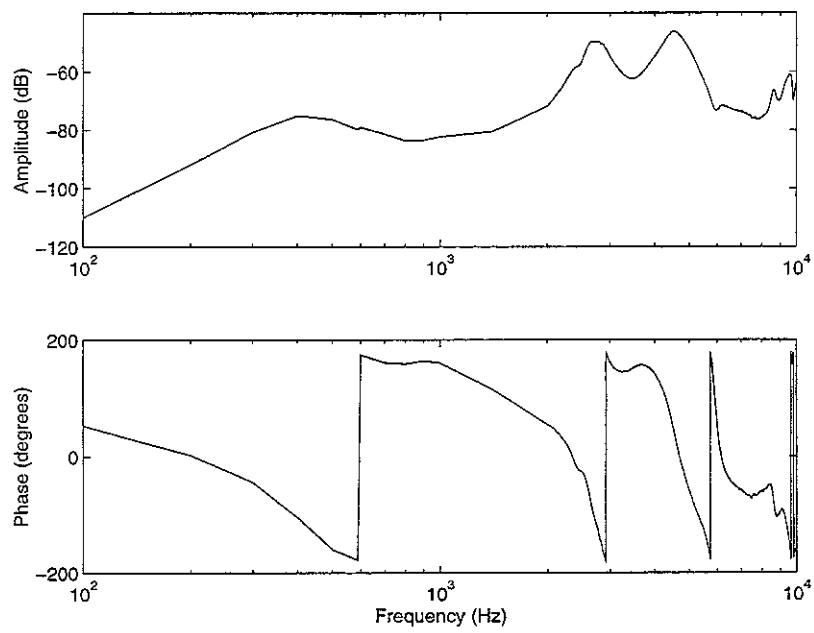
## Figure 3
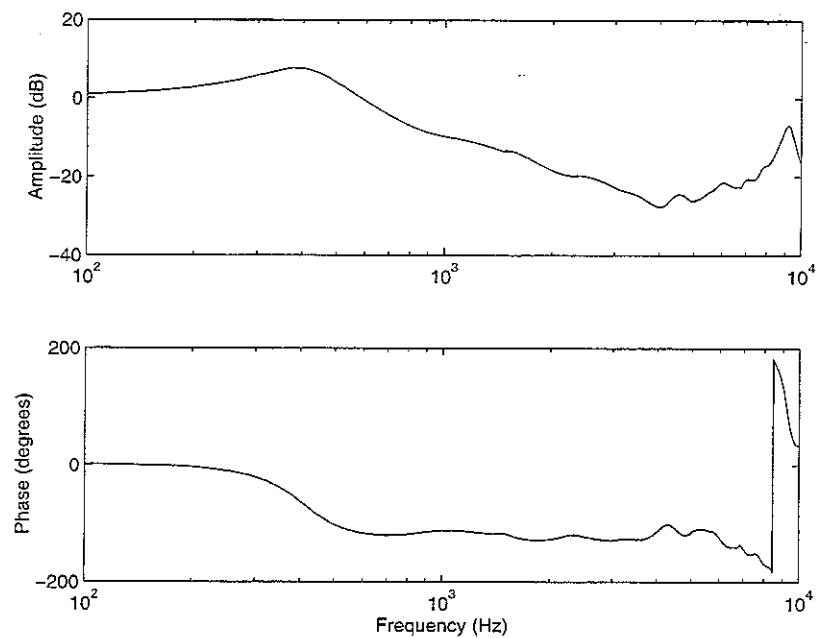
Figure 4
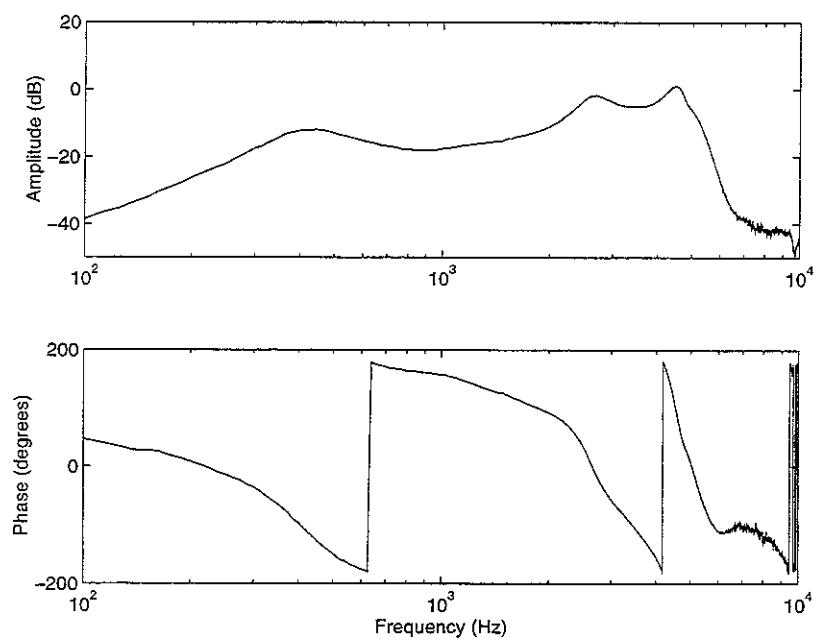
Figure 5

Figure 6

Figure 7
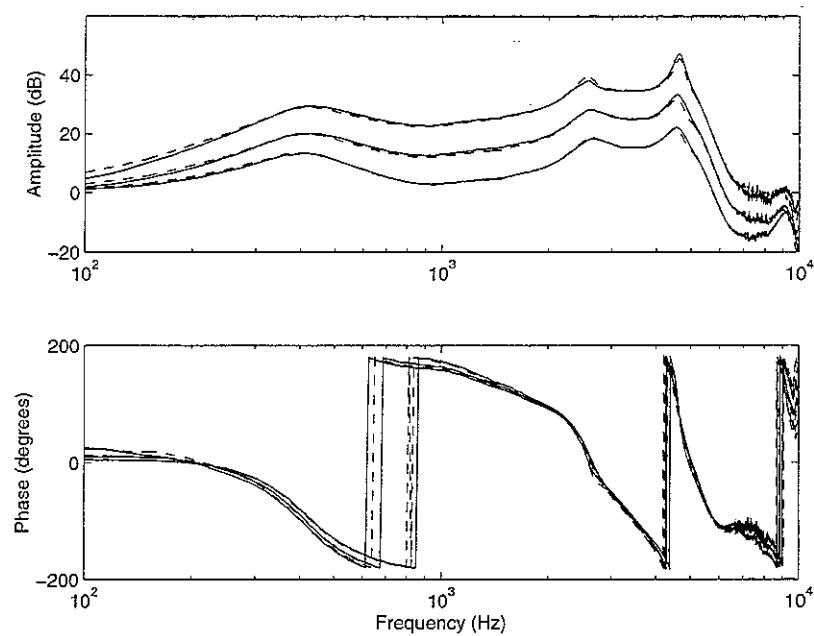
**Figure 8**
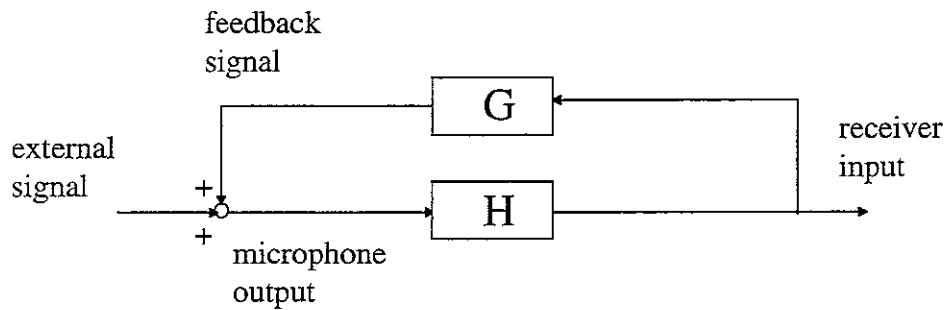
Figure 9
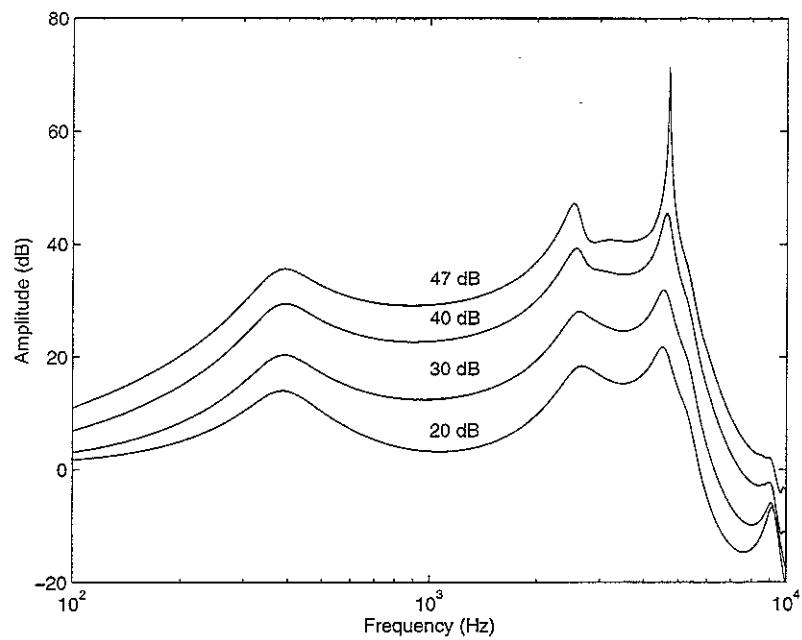
Figure 10
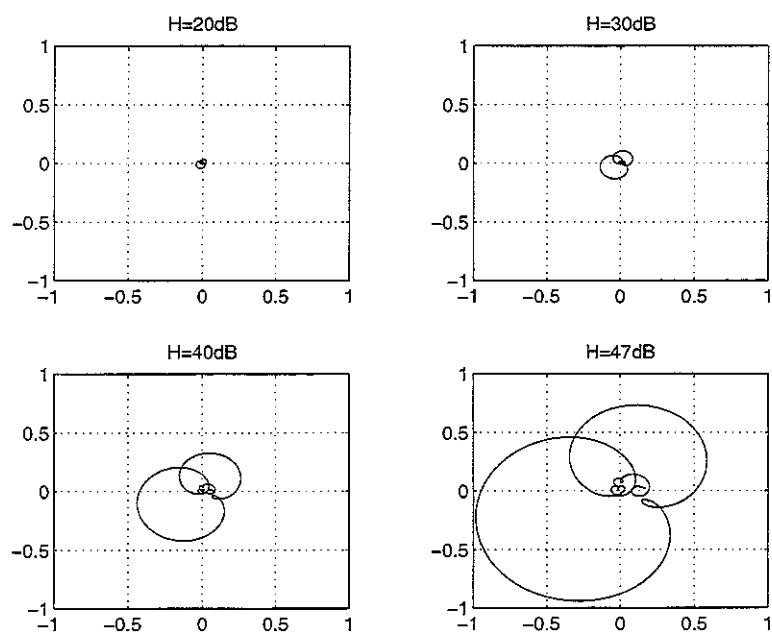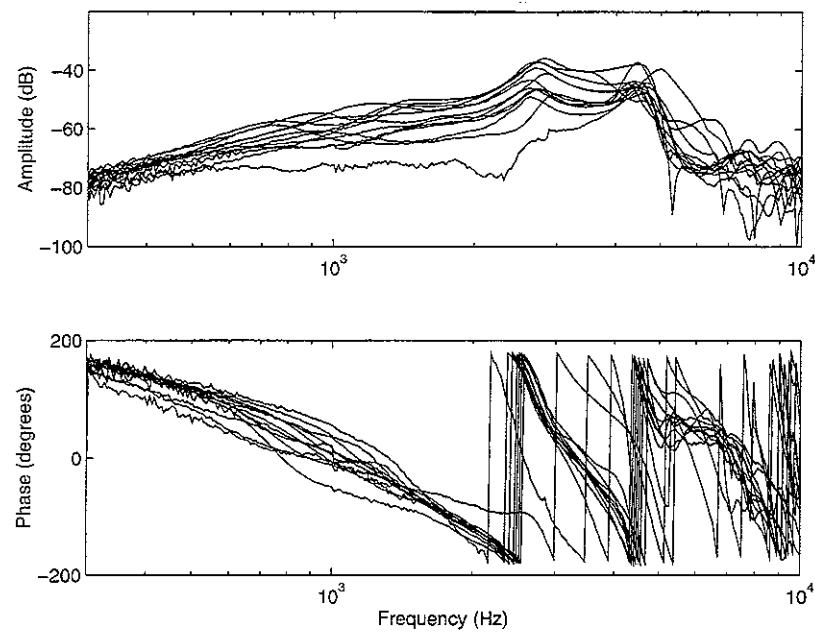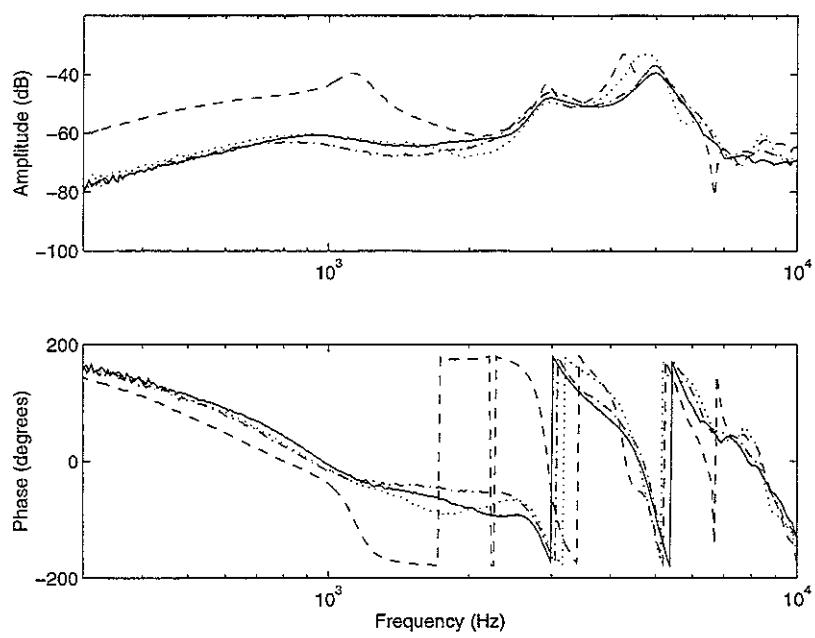
Figure 11
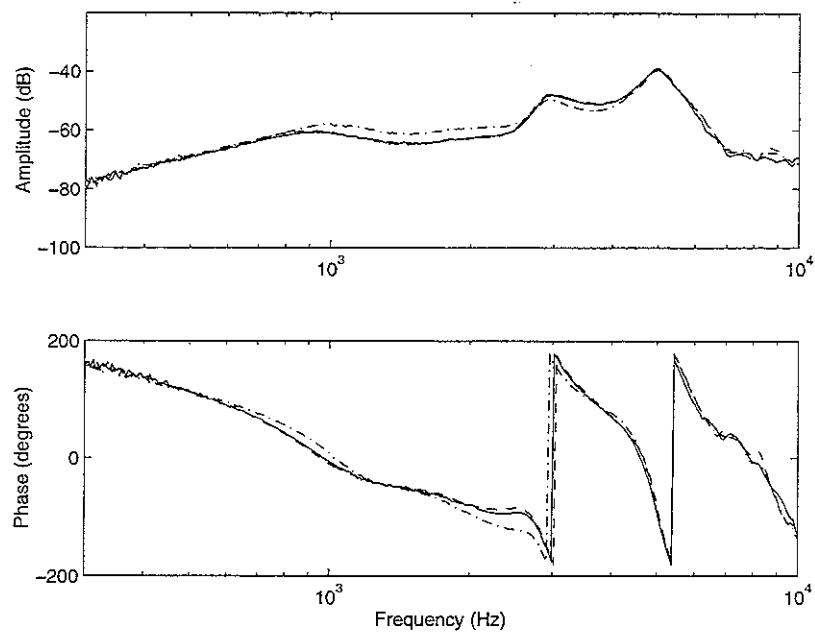
Figure 12

Figure 13

Figure 14

Figure 15

Figure 16

Figure 17

-$G_0(j\omega)H(j\omega)$

|$G_0(j\omega)H(j\omega)$|$W(\omega)$
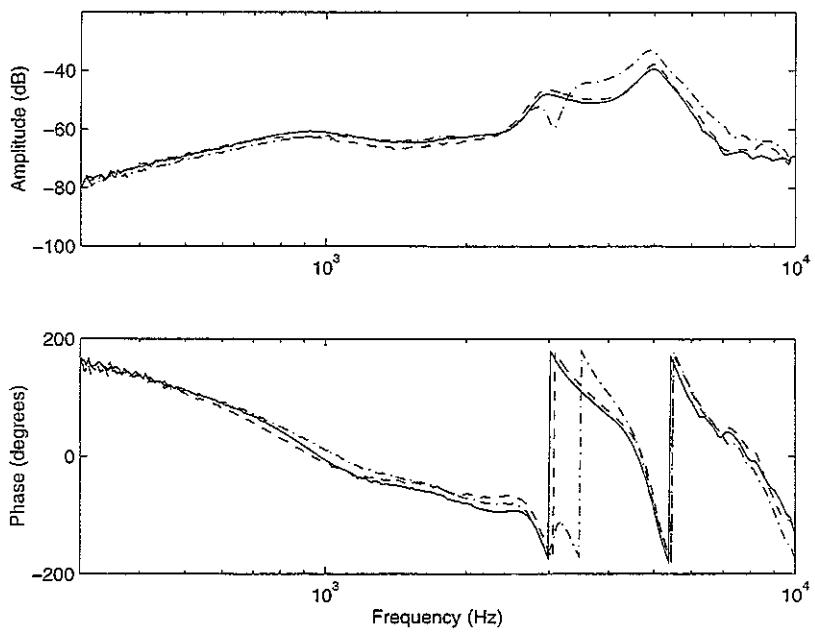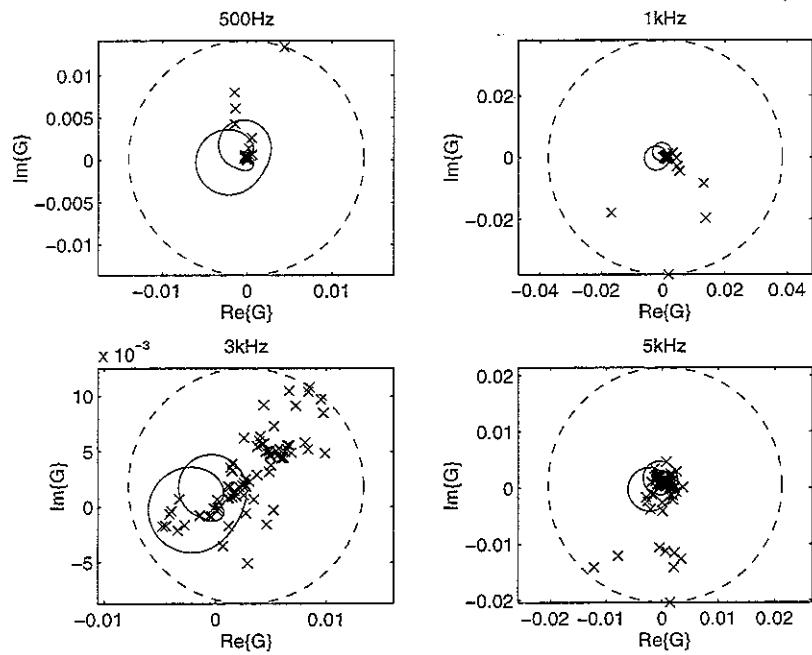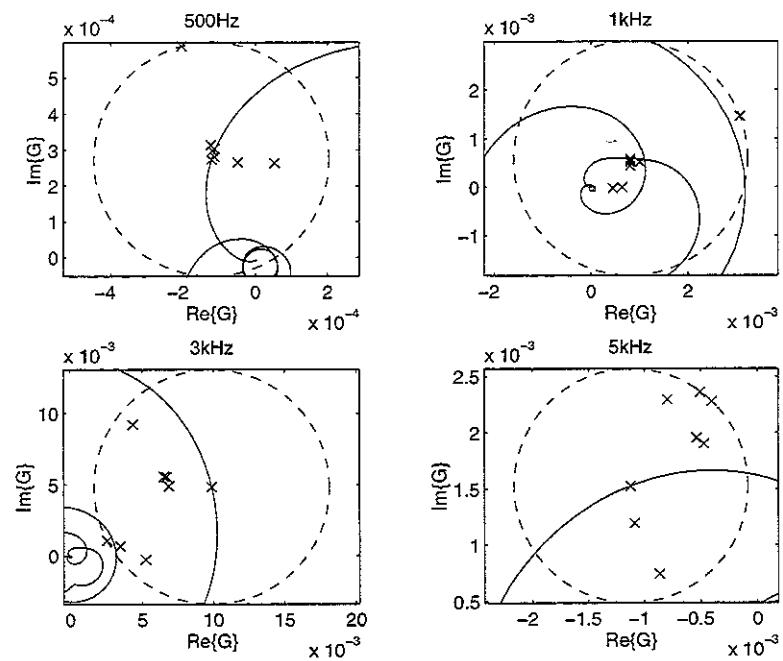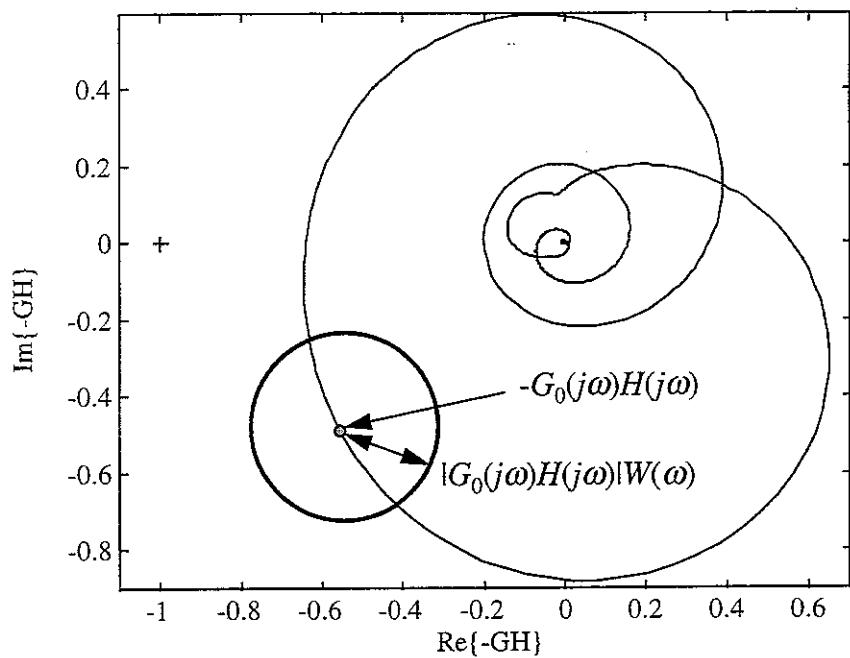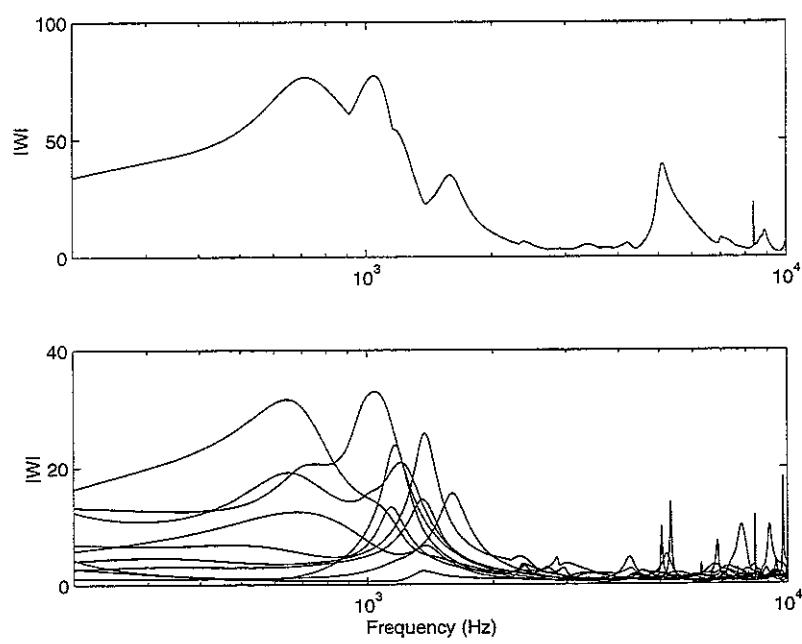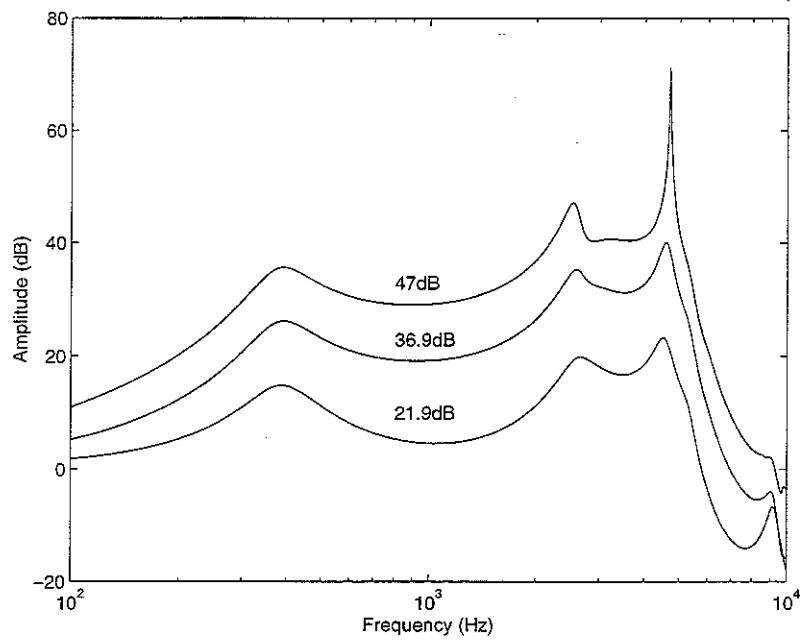
Figure 18

Figure 19

Figure 20
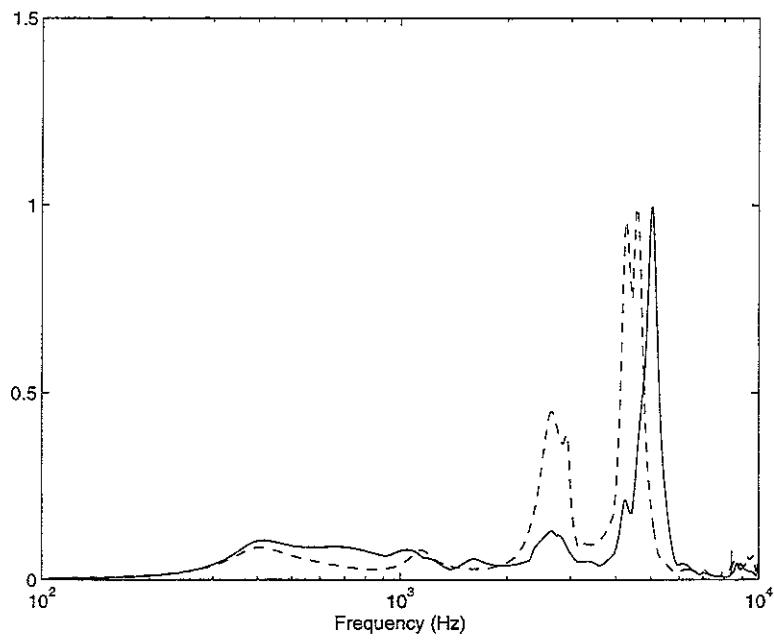
Figure 21
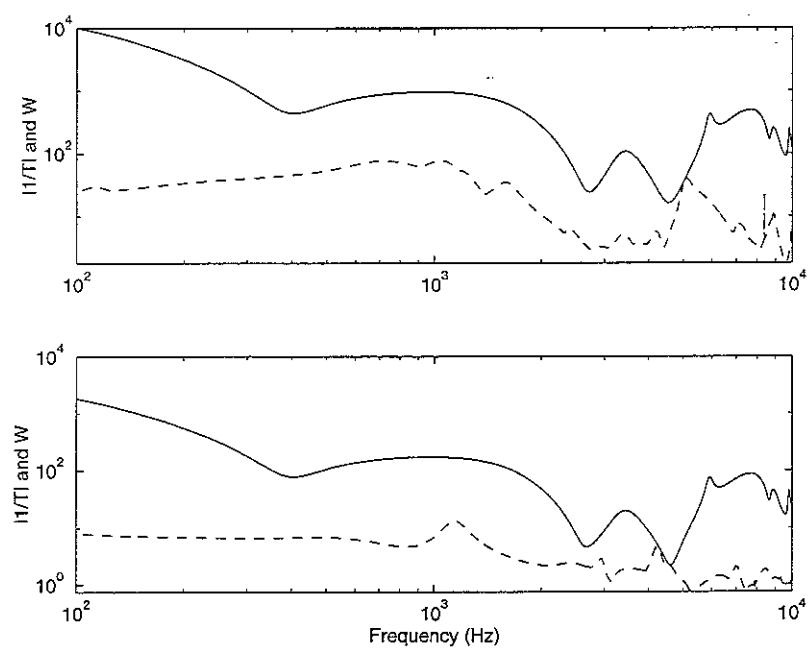
Control of feedback in hearing aids - a robust filter design approach

B. Rafaely and M. Roccasalva Firenze

Institute of Sound and Vibration Research, University of Southampton, Highfield,

Southampton, SO17 1BJ, UK

Corresponding author:

Boaz Rafaely

Institute of Sound and Vibration Research

University of Southampton,

Southampton, SO17 1BJ

UK

Email: br@isvr.soton.ac.uk

Tel: +44 (0)1703 593043

Fax: +44 (0)1703 593190

ABSTRACT

Many hearing aids users suffer from feedback, which cause the hearing aid to whistle or howl when the conditions of use are varied, for example when a hand is placed near the ear. Some digital hearing aids use feedback cancellation filters to reduce the feedback signal and so control the feedback problem. This paper presents a new approach to designing digital hearing aid filters, which makes the stability of the system robust to variations in the feedback path and thus avoids the feedback problem. This approach can be used for digital hearing aids with both fixed or adaptive feedback cancellation filters. First, a model of the uncertainty in the feedback path is introduced, which is then used to design digital filters that meet a required compensation response, while maintaining robust stability. Both FIR and sub-band filters are designed using data measured from a commercial hearing aid.

I. INTRODUCTION

Digital hearing aids are becoming increasingly popular, with new digital signal processing (DSP) technology enabling smaller and lower power hearing aids with improved performance to be implemented in in-the-ear and in-the-canal configurations. The feedback problem, which cause the "howling" or "whistling" sound when the receiver signal is fed-back to the microphone, is also easier to handle in digital hearing aids. Adaptive feedback cancellation algorithms has been developed and tested, which

cancel the feedback signal using an internal model of the feedback path. Many of these algorithms are useful in reducing the level of the feedback signal, thus allowing for higher gain and improved performance before the hearing aid approaches instability [1]-[6].

One of the limiting factors of the adaptive feedback cancellation approach is that the feedback path model is never perfect, and so a residual feedback signal still exists which hinder any additional gain. The variability of the feedback path in various hearing aid fittings and conditions is a major contributor to the discrepancy between the feedback path and its digital model. Maxwell and Zurek [1] suggested studying the variability of the feedback path as a function of time under different conditions, to support the design of adaptive filters that track these changes. Siqueira *et al* [2] studied these variations, with a hand approaching the ear, for example, and tested adaptive algorithms that would track these changes. Even with improved adaptive algorithms, perfect cancellation of the feedback signal is impossible to achieve if the variability occurs more quickly than the convergence speed of the adaptive algorithm. In this case, the hearing aid system must be made *robust* to any variations in the feedback path which are not accounted for by the model, otherwise the system will go unstable.

This study presents a new approach in the design of hearing aid filters which are robust to any given uncertainty in the feedback path thus avoiding the feedback problem. This approach can be used in digital hearing aids with a fixed cancellation filter, to ensure stability in the face of feedback path uncertainty, or in digital hearing aids with adaptive cancellation filter, to ensure stability in the face of variations in the feedback path which cannot be tracked by the adaptive filter. Furthermore, an integrated approach is used in

the design of the hearing aid filter to compute a filter that meets the required compensation, or amplification response, while maintaining robust stability in the face of feedback path variations.

The paper is organised as follows. Section II presents the hearing aid used in this study and the model used to describe the measured feedback path variability. Section III presents the robust stability condition, and section IV illustrates how this condition is used to define the limit of the compensation filter magnitude. Section V outlines four different methods for designing robust compensation filters, and section VI presents simulation results of the hearing aid performance with the various designs.

II. FEEDBACK IN HEARING AIDS

A typical hearing aid includes a microphone to detect the external sound, an amplification filter to provide the required compensation, and a receiver which transmits the amplified sound into the user's ear canal. A vent connecting the ear canal to the outside is usually also fitted, to reduce the unnatural feeling induced when the ear is occluded. Hearing aid systems have been studied previously through simulations and measurements [8]-[9], where the acoustic and electrical mechanisms involved were carefully analysed. A block diagram of a typical hearing aid systems is presented in Figure 1, where M and R are the electroacoustic response functions of the microphone and the receiver, respectively, B and A are the acoustic response functions of the vent, from the ear canal, and from the outside,

respectively, G is the electrical frequency response of the feedback path, from the receiver input to the microphone output, and H is the amplification filter.

Acoustic feedback occurs when the sound generated by the receiver inside the ear canal is fed-back to the microphone through the vent. Although other forms of feedback exist, such as mechanical and electrical feedback, the acoustic feedback is usually the main cause for the howling and whistling problem.

An in-the-ear hearing aid (Starkey 11M) was used in this work, with the amplifier disconnected to allow direct access to the transducers. A comprehensive experiment was recently conducted using this hearing aid [10] to study the acoustic feedback path and its variability under different conditions. It was found that large variability occurs between ears and subjects, and when placing a hand very close to the ear or when fitting the hearing aid incorrectly. More moderate variations occurred under other conditions such as head and face movements and a when a hand was placed further away from the ear.

The variations in the frequency response of the feedback path found in [10] were compared to the response measured with a normal hearing aid fit under normal conditions, referred to as the nominal response. It was shown that the variations, when analysed in the complex Nyquist plane, tend to spread relatively randomly around the nominal values, particularly at high frequencies. The multiplicative uncertainty model, widely used in robust control [11] was then used to describe the bound of these variations around the nominal value. The resulting bound is a circle in the Nyquist plane around the nominal value. Although it might produce a conservative description of the uncertainty

when the actual variations do not completely fill that circle, it does leads to a simple and useful stability condition. Figure 2 illustrates a Nyquist plot of the feedback path under normal conditions (solid curve), with the variations in the feedback path at 5.3kHz marked by "x", enclosed by the circular uncertainty bound, showing that the various values are reasonably spread inside the circle.

The multiplicative uncertainty bound can computed by first writing the response of any feedback path G in terms of the nominal response G_0 as:

$$G = G_0(1 + \Delta) \tag{1}$$

where Δ is a complex function of frequency. The multiplicative uncertainty bound W of any G from the set $\tilde{G}$ around G_0 is then defined as:

$$W = \max_{G \in \tilde{G}} |\Delta| = \max_{G \in \tilde{G}} \left| \frac{G}{G_0} - 1 \right| \tag{2}$$

which defines a circle of uncertainty around the nominal value on the Nyquist plane, as illustrated in Figure 2, with G_0 the circle centre and $|WG_0|$ the circle radius. The measurement sets $\tilde{G}$ in this work included various conditions, such as placing a hand near the ear, incorrect hearing aid fitting, and face movements for an individual ear. It should be noted that large inter-subject variability was measured in [10], but this is not included here since it is assumed that the hearing aid is customised to each ear, so that any uncertainty in the feedback path due to inter-subject variability can be ignored.

Figure 3 shows the multiplicative uncertainty bounds W calculated using equation (2) for the data measured in [10], with the measurement set including various conditions for one ear. The frequency response of the feedback path for that ear under normal conditions was chosen as the nominal response G_0 when calculating W. Figure 3 shows that large uncertainty in the feedback path exists at low frequencies, which is primarily due to the condition with a hand very close to the ear, while smaller uncertainty is observed at high frequencies, which is due to the other conditions [10].

III. ROBUST STABILITY

The results obtained above are used in this work to design hearing aid filters that are robust to a given uncertainty in the feedback path, and therefore do not suffer from howling under the given conditions. As suggested in [10] and used in robust control design methods [11], a condition for robust stability which uses the multiplicative uncertainty bound can be written as:

$$|WT_0| < 1 \qquad \text{for all } \omega \tag{3}$$

where T_0 is the nominal complementary sensitivity function given by $G_0H/(1-G_0H)$ in this case. This condition can be written using the ∞-norm [11] as:

$$\|WT_0\|_\infty < 1 \tag{4}$$

An Internal Model Control (IMC) [12], widely used in many feedback control design methods to simplify the design process [13],[14] is used here to parametrise the filter H using a filter Q and a feedback path model G_0, as shown in Figure 4. The hearing aid filter H is can now written as:

$$H = \frac{Q}{1 + QG_0}$$
(5)

Figure 4 also represents the block diagram of a hearing aid system which uses feedback cancellation to reduce the effect of feedback, assuming $G_0 \approx G$. The strong similarity between IMC and adaptive feedback cancellation is used in this work to generalise the feedback cancellation technique into a robust filter design framework.

The robust stability condition in equation (4) can now be written in terms of the filters Q and the model G_0 using equation (5) as [12]:

$$\|WQG_0\|_\infty < 1$$
(6)

Equation (6) states that the hearing aid system will be robust to variations in the feedback path, as long as these variations around the nominal value G_0 are bounded by W, and that Q is chosen to satisfy equation (6). For an adaptive model G_0 in an adaptive feedback cancellation scheme, the actual variations of the feedback path from the model can be reduced by tracking the feedback path response, such that the resulting W is smaller. Since most feedback systems have an inherent trade-off between performance and robust

8

stability [11], smaller W will usually allow better performance. Given G_0 and W, filter Q can be designed to be robust to the given variations, as shown below.

The formulation described above is used to guarantee robust stability. In practice, however, large enhancement might occur before instability is reached, if the stability margins are very small, so a larger W than computed by equation (2) might be required to prevent howling. Nevertheless, in this work equation (2) is used to compute W. The exact increase in W required in practice to prevent howling is proposed for future work.

IV. A LIMIT ON COMPENSATION GAIN

Hearing aids are designed primarily to provide compensation for hearing loss, and digital hearing aids provide the flexibility required in the implementation of the hearing aid filters to improve that compensation. In the next two sections it is shown how accurate compensation and robust stability in the face of variations in the feedback path can be achieved simultaneously in a unified design framework.

The hearing loss of hearing impaired patients is measured using an audiometric test, which defines the increase in the level of the threshold of hearing in the audio frequency range. Then, a hearing aid is fitted and its gain adjusted to compensate for the hearing loss. A correct frequency shaping of the hearing aid filter will ensure better compensation and improved performance from the hearing aid. In many digital hearing aids, the

response of the hearing aid filter can be programmed by the audiologist, thus making the hearing aid customisation process faster and better.

The magnitude of the compensation filter Q shown in Figure 4, is therefore set to a given frequency response, denoted by C, which is calculated from the result of the audiometric test and the specifications of the given hearing aid, usually to allow comfortable levels for normal speech. However, when the hearing loss is sever, and the response of C involves high gain levels, the stability margins in the face of variations in the hearing aid feedback path may not be sufficient, and the hearing aid might suffer from "howling". In this case the gain of the hearing aid is usually reduced to avoid howling, but on the expense of performance.

The requirement for compensation and the condition for robust stability can be written simultaneously as:

$$|Q| = C \text{ and } |WQG_0| < 1 \quad \text{for all } \omega \tag{7}$$

which can be rewritten as:

$$|Q| = C \text{ and } |Q| < 1/|WG_0| \quad \text{for all } \omega \tag{8}$$

Since both of these conditions are on the magnitude of Q, they can be combined into a single equation which determine the magnitude of Q as follows:

$$|Q| = \min\left(C, \frac{1}{|WG_0|} \right) \quad \text{for all } \omega \tag{9}$$

Equation (9) suggests that the magnitude of Q at each frequency should be set to the required compensation level C, as long as $C < 1/|WG_0|$, but is limited by $1/|WG_0|$ otherwise. The term $1/|WG_0|$ therefore acts as a *gain limit*, indicating the maximum gain a compensation filter can achieve if it was to be robust to variations in the feedback path. This is a useful measure, which can be derived directly from measurements of the feedback path under normal conditions, G_0, and the bound of the variations under all other conditions, W.

Figure 5 shows the magnitude of a required compensation C, which was simply set to a constant gain of 55dB in this case, and the magnitude limit $1/|WG_0|$ which was calculated for one ear from the measurements reported in [10]. The figure clearly show that there is a limit on the magnitude of the compensation if robust stability is to be maintained, and that in this case the required compensation could not be achieved at frequencies between about 2kHz and 6kHz.

V. DESIGN OF ROBUST COMPENSATORS

The design methods described below show how a compensation filter Q with a magnitude which is as close as possible to the required compensation magnitude C can be designed, which also maintains the required robust stability condition.

1. Design of a linear-phase FIR filter

A simple design procedure for the filter Q can be formulated in the frequency domain, assuming the compensation filter Q has a sufficient frequency resolution, which could be achieved by a long FIR filter for example. First, the magnitude of the filter is computed using equation (9), and then the FIR filter coefficients are computed using a direct inverse Fourier transform of the magnitude Q. Since the quantities in equation (9) are computed from measured data which normally involved functions of discrete frequency, it is assumed below that C, W and G_0 are all functions of a discrete frequency index k, with a sufficiently high frequency resolution to produce an accurate representation of the continuous problem. This approach was previously used in feedback control design [15], where it was argued that this approximation is reasonable as long as the number of discrete frequency points is sufficiently large to capture the complete time response of the frequency variables and to avoid circular convolution effects in frequency domain operations.

Denoting q as the coefficient vector of an FIR filter of length N, the design procedure is outlined below.

a) Compute the magnitude of the compensation filter $|Q| = \min\left(C, 1/|WG_0|\right)$.

b) Compute the FIR filter $q = DFT^{-1}\left\{|Q|\right\}$.

c) Truncate any zero of negligible coefficients, to a length of I.

12

where DFT denotes the Discrete Fourier Transform. The FIR filter computed in step (b) is symmetric since $|Q|$ is real, and is non-causal since $|Q|$ has zero phase. For q to be implemented, it has to be delayed by $I/2$ samples, where I is the filter length after truncating any zero or negligible coefficients. The resulting FIR filter is therefore linear-phase symmetric FIR filter. Although it might have a long delay, it will not produce any phase distortion to the hearing aid signal.

2. Design of a minimum-phase FIR filter

An alternative method to design an FIR filter given the magnitude of Q is by computing the minimum-phase corresponding to the magnitude of Q, which is done here using the Cepstrum transform [19]. The design procedure is outlined below.

a) Compute the magnitude of the compensation filter $|Q| = \min(C, 1/|WG_0|)$.

b) Compute the FIR filter $q = DFT^{-1}\left\{exp\left(DFT\left\{wDFT^{-1}\left\{log|Q|\right\}\right\}\right)\right\}$.

c) Truncate any zero of negligible coefficients, to a length of I.

In step (b) the filter is transformed to the Cepstrum domain, and its non-causal part truncated using an appropriate causal window w [19], and then transform back to the time domain using inverse-Cepstrum operation. The resulting FIR filter is causal and minimum-phase, and has the advantages of small phase changes, although these are not linear. Since it is a causal filter, it can be implemented directly.

3. Design of an FIR filter via constrained optimisation

The two design methods described above assumed that the FIR filters are long enough to allow an accurate implementation of a desired magnitude response. However, a short FIR filter is often desirable due to DSP hardware constraints. In this section a constrained optimisation approach is used to design an FIR filter of any desired length, which will result in a compensation magnitude as close an possible to the required magnitude C, while maintaining robust stability. The objective of designing Q similar to C can be written as minimising the mean square error between the two, and together with the robust stability condition, a constrained optimisation problem can be written as:

$$\min_{q} \sum_{k=0}^{N-1} |Q(k) - C(k)|^2 \tag{10}$$

$$\text{subject to } |W(k)Q(k)G_0(k)|^2 < 1 \qquad k=0...N\text{-}1$$

where N is the number of frequency points, and q is an FIR filter related to $Q(k)$ by:

$$Q(k) = \sum_{i=0}^{N-1} q_i e^{-j2\pi k/N} = q^T e(k) \tag{11}$$

where $e(k)$ is a complex vector of the DFT coefficients. It should be noticed that the value $Q(k)$ was used in equation (10), rather than the magnitude $|Q(k)|$, since it was assumed that q is a symmetric non-causal filter, such that its Discrete Fourier Transform $Q(k)$ is

entirely real. This simplifies the formulation of the optimisation problem, although before

implementation, an appropriate delay has to added to q to transform it to a causal filter.

This formulation is used so that the optimisation problem will be convex, and thus have a

unique minimum. The objective term $|Q(k) - C(k)|^2$ in equation (10) can be written for

each frequency k using equation (11) in the quadratic form $q^T A q + q^T b + c$ which is

convex provided the matrix A is positive semidefinite [18]. This is true since

$q^T A q = |Q(k)|^2 \geq 0$ for all q, and the term $|Q(k) - C(k)|^2$ is therefore convex. The

additional summations in equation (10) are convex operations, so the entire objective

term in equation (10) is convex. The constraint terms in equation (10) can also be written

as $q^T A q = |WQG_0|^2 \geq 0$ for all q, and the same convexity argument is followed here to

show that all the constraints are convex. Therefore, the complete constrained optimisation

problem as presented in equation (10) is convex [16], with a unique minimum value, and

can be solved for the optimal q. In practice, a sequential quadratic programming (SQP)

solver implemented by the Matlab function *constr()* was used in this work.

It should be noted that if a non symmetric FIR was to be used, the optimisation problem

would not be necessarily convex, since an objective term $||Q(k)| - C(k)|^2$ would have to

be used, which will only be convex if the term $|Q(k)| - C(k)$ is monotonic in q [18],

which is generally not true. In this case non-convex optimisation solvers should be used.

4. Design of sub-band filters

Another method is presented below for designing a sub-band compensation filer in the frequency domain. In this case, the compensation filter is composed of band pass filters, with the gain value of each sub-band filter increased until the desired compensation level is achieved, or until the robust stability condition is no longer maintained. With this filter architecture accurate compensation at a wide frequency range could only be achieved with large number of sub-band filters, which will produce the required frequency resolution.

The sub-band filter, commonly used in audio applications can be written as a function of the gain vector a of the individual band-pass filters as:

$$Q(k) = \sum_{i=0}^{I-1} a_i S_i(k) = a^T S(k) \tag{12}$$

where $S_i(k)$ is the frequency response of the band-pass filter in the i-th band having a gain of a_i. A simple design procedure would be to set the gain a_i according to the corresponding gain specified by equation (9), where the i-th frequency represents the centre frequency of the band pass filter. Then the magnitude of each sub-band can be adjusted to comply with the robust stability condition, if necessary. Alternatively, a more accurate design procedure can be formulated using constrained optimisation, in a similar way to the design of the FIR filter described above, in which case the optimisation parameter will be the vector a.

VI. SIMULATION RESULTS

The filter design frameworks described above were used to design both FIR and sub-band robust compensation filters using the measured hearing aid data described in section II. The response of the hearing aid from the pressure outside the ear to the pressure in the ear canal, was then computed for each compensation filter. This response can be written using Figure 1 as:

$$\frac{P_{ear}}{P_{ext}} = A + \frac{MHR}{1 + GH} \qquad (13)$$

With the filter H configured using IMC as in equation (5), with G_0 equal to the hearing aid feedback path response under normal conditions G, equation (13) can be written as:

$$\frac{P_{ear}}{P_{ext}} = A + MRQ \qquad (14)$$

This equation was used to calculate the hearing aid response for a given computed compensation filter Q, given A, M and R as measured for the in-the-ear hearing aid used in this work. Figure 6 shows the frequency response of the feedback path G as used in the simulations below, showing high frequency peaks due to the response of the hearing aid receiver. Figure 7 shows the frequency response of the acoustic path A (solid curve), which has a peak at around 400Hz, due to the vent inertia and the ear canal compliance, and another peak at around 9kHz due to standing waves in the vent. The frequency response of $M \cdot R$, which is the transducers response, is also illustrated (dashed curve), showing high frequency peaks due to the response of the receiver.

The feedback path uncertainty bound W used in the simulation was a bound measured for one ear, as discussed above. In the first design example, a linear-phase FIR filter was designed through the frequency domain method described in section V.1. A sampling frequency of 25.6kHz was used with Fast Fourier Transform (FFT) size of 2048. After computing the FIR filters q, the frequency response of the hearing aid was computed using equation (14). As a simple design example, C, the desired compensation response, was chosen as a constant gain of 55dB, giving an overall high-pass response for the hearing aid due to the response of the transducers. The results could then be compared to the performance achieved by a constant gain amplifier (constant G in Figure 1) designed with maximum gain while maintaining the robust stability constraint as in equation (3).

Figure 8 shows the overall frequency response of the hearing aid from external pressure to internal pressure with the FIR filter (solid curve) and the constant amplification compensator (dashed curve), which shows that a much higher gain can be achieved with the FIR filter compared to the constant amplification filter. The explanation for this can be found by considering the frequency response of the FIR filter Q (solid curve) compared to the magnitude of the constant gain filter G (dashed curve) as shown in Figure 9. The FIR filter achieved the desired magnitude of 55dB at most frequencies, except at two high frequency bands, where the robust stability condition constrained the magnitude to lower values. The constant gain compensator G, however, was bounded to a gain of about 37dB above which robust stability was not maintained. The improved performance of the FIR filter was therefore achieved by allowing increased gains at frequencies where robust stability was not compromised.

Figure 10 emphasise the difference between the FIR and the constant gain filter, where the robust stability term $|WQG_0|$ is compared to $|W G_0 H/(1 - G_0 H)|$ for both designs. The Figure shows that both designs maintained robust stability, with the robust stability term smaller than one. However, the design with the FIR filter is less conservative and approaches nearer the robust stability bound, therefore achieving better performance, a trade-off widely recognised in the design of robust feedback controllers [11]. Figure 11 shows the impulse response of the linear-phase FIR filter, having a total length of 309 samples, and a delay of 154 samples.

A minimum-phase FIR filter was designed next, following the procedure described in section V.2, and was compared to the linear-phase FIR filter designed above. Figure 12 shows the hearing aid frequency response with the two designs, illustrating that a similar performance was achieved in both cases. Figure 13 shows the impulse response of the minimum-phase FIR filter, showing that a shorter filter, with only 128 coefficients, could be implemented in this case. The advantages of the minimum-phase FIR filter, are a potentially shorter impulse response, and no delay. The linear-phase filter has a long delay, although its phase is linear. The linear-phase is not a significant advantage, however, since some phase distortion is introduced anyway by the transducers, and moreover the ear is not very sensitive to phase distortion.

In some digital implementations it is important to design a short FIR filter for easier real-time realisation. The following design follows the procedure suggested in section V.3 which uses constrained optimisation to design a linear-phase FIR filter with 31

coefficients. Figure 14 shows the overall hearing aid response with the FIR filter designed using constrained optimisation, compared to the hearing aid response with the linear-phase FIR filter design as in section V.3. Differences of about 5dB are observed at some frequencies but the responses are generally similar. Figure 15 illustrates the magnitude response of the two FIR filters, showing that the short FIR filter doesn't accurately approximate the required magnitude response, although the variations from the required gain are not very large. It should be noted that designing a shorter FIR filter by simply truncating the long linear-phase FIR filter is not a desirable design method, since the truncation will not guarantee that the robust stability constraint is be maintained. In this case the optimisation procedure is necessary to ensure robust stability.

The last design involved sub-band filters, as proposed in section V.4. The sub-band filter was composed of a set of 20 FIR band-pass filters, each with 200 coefficients, linearly spaced over the complete frequency rage, thus having a bandwidth of 500Hz each. Figure 16 shows the hearing aid response with the sub-band filter compared to the linear-phase FIR filter designed according to section V.4, and Figure 16 compares the magnitude response of the two filters. The sub-band filter achieves a magnitude similar to the linear-phase filter at most frequencies, with a resulting similar performance. The advantage of the sub-band filter is its more direct design, where the gain at each band can be set directly to the maximum allowed gain. Figure 18 shows the separate sub-band filter with their relative amplitudes.

The design methods described above require the estimation of the uncertainty bound W for a given ear. Although developing a method for estimating W during the hearing aid

customisation process is left as a topic for future research, Figure 19 shows the robust stability magnitude bound $1/|WG_0|$ for several different ears measured in [10]. Although the bounds are different for each ear, they do seem to have a similar frequency shape. It may be possible to use this similarity to simplify the procedure for computing W for each ear.

CONCLUSIONS

A new approach in designing digital hearing aid filters was presented in this paper. A multiplicative bound on the feedback path variations was used to formulate design methods for digital filters that accurately achieve the required compensation response, while maintaining robust stability in the face of feedback path variations, thus avoiding howling. It was shown that given the response of the feedback path and the bound on the variations, the limit on the magnitude of the compensation filter can be determined. This is a useful measure to predict the maximum compensation gain before howling occurs.

Four design methods were proposed and performed on data measured from commercial hearing aid. These involved linear-phase and minimum-phase FIR filters, and sub-band filters, using design in the frequency domain and via constrained optimisation.

The development of a method to compute the uncertainty bound during the hearing aid customisation process, and the integration of the robust design methods in digital hearing aid filters, both for fixed and adaptive systems, are proposed for future research.

REFERENCES

[1]   J. A. Maxwell and P. M. Zurek, "Reducing Acoustic Feedback in Hearing Aids,"
        IEEE Transactions on Speech and Audio Processing, 3(4), 304-313, 1995.

[2]   M. G. Siqueira, R. Speece, E. Petsalis, A. Alwan, S. Soli, and S. Gao, "Sub-band
        Adaptive Filtering Applied to Acoustic Feedback Reduction in Hearing Aids,"
        Proceedings of the IEEE Asilomar Conference on Signals, Systems and
        Computers, November, 1996.

[3]   R. Wang and R. Harjani, "Acoustic Feedback Cancellation in Hearing Aids,"
        Proceedings of the IEEE International Conference on Acoustics, Speech and
        Signal Processing, 137-140, 1993 .

[4]   H.A.L. Joson, F. Asano, Y. Suzuki, and T. Sone, "Adaptive feedback cancellation
        with frequency compression for hearing aids", J. Acoust. Soc. Am. 94 (6), 3248-
        3254, 1993.

[5]   S. Wyrsch, A. Kaelin, "A DSP implementation of a digital hearing aid with
        recruitment of loudness compensation and acoustic echo cancellation", Workshop
        on application of signal processing to audio and acoustic, New Paltz, New York,
        19-22 October, 1997.

[6]   J.M. Kates, "Feedback cancellation in Hearing Aids: Results from a computer
        simulation", IEEE Transaction on Signal Processing, 39(3), 553-562, 1991.

[7]   D. A. Preves, J. A. Sigelman and Philip R. LeMay, "A Feedback Stabilizing
        Circuit for Hearing Aids," Hearing Instruments, 37(4), 35-41, 1986.

[8]   D.P. Egolf, H.C. Howell, K.A. Weaver and D.S. Barker, "The hearing aid
        feedback path: Mathematical simulations and experimental verification", J.
        Acoust. Soc. Am. 78 (5), 1578-1587, 1985.

[9]   J.M. Kates, "A computer simulation of hearing aid response and the effects of ear
        canal size", J. Acoust. Soc. Am. 83(5), 1952-1963, 1988.

[10]   M. Roccasalva-Firenze, B. Rafaely and E. Payne, "Feedback path variability in

hearing aids", submitted to the J. Acoust. Soc. Am., 1999.

[11]   S. Skogestad and I. Postlethwaite, Multivariable Feedback Control, John Wiley & Sons, 1996.

[12]   Morari, M. and Zafiriou, E. (1989). Robust process control. Prentice-Hall, NJ.

[13]   Newton, G.C., Gould, L.A., Kaiser, J.F. (1957). Analytical design of linear feedback controls. John Wiley & Sons, NY.

[14]   Elliott, S.J., Sutton, T.J., Rafaely, B. and Johnson, M. (1995). "Design of feedback controllers using a feedforward approach". *Proceedings of the ACTIVE95 conference*, 863-874, CA, USA.

[15]   Rafaely, B. and Elliott, S.J., (1999) "H2/H-infinity active control of sound in a Headrest: design and implementation," *IEEE Transactions on Control Systems Technology*, 7(1), 79-84.

[16]   Fletcher, R. (1987). Practical methods of optimization. John Wiley & Sons.

[17]   Gill, P.E., Murray, W. and Wright, M.H. (1981). Practical optimization. Academic Press.

[18]   Roberts, A.W. and Varberg, D.E. (1973). *Convex Functions*. Academic Press

[19]   Oppenheim A.V. and Schafer R.W. (1975). *Digital Signal Processing*. Prentice-Hall International.

FIGURE CAPTIONS

Figure 1 A block diagram of a typical hearing aid system.

Figure 2 A Nyquist plot of the feedback path under normal conditions (solid curve), the response values under other conditions for that ear at 5.3kHz, marked by "x", and enclosed by the circular uncertainty bound (dashed curve).

Figure 3 The multiplicative uncertainty bound W for one ear calculated for variations in the feedback path under various measurement conditions.

Figure 4 A block diagram of the feedback path G and the compensation filter H, implemented as an Internal Model Controller using filter Q and a feedback path model G_0.

Figure 5 The magnitude of $1/|WG_0|$ (solid curve) which represents the maximum allowed gain for Q which still complies with the robust stability condition. As an example, a required gain of 55dB is introduced, illustrating the frequency range where it cannot be met due to the robust stability condition.

Figure 6 The frequency response of the feedback path G as used in the design simulation.

Figure 7 The frequency response of the acoustic path A from outside the ear into the ear canal (solid curve), and the frequency response of the transducers $M \cdot R$ (dashed curve), as used in the design simulations.

Figure 8 The frequency response of the hearing aid, P_{ear}/P_{ext}, with the linear-phase FIR filter (solid curve) and the constant gain compensator (dashed curve).

Figure 9 The magnitude response of the linear-phase FIR filter Q (solid curve) and the constant gain compensator H (dashed curve).

Figure 10 The robust stability constraint term for the hearing aid systems with the linear-phase FIR filter, $|WQG_0|$ (solid curve), and for the systems with the constant gain filter,

$\left| W\,G_0H/(1-G_0H) \right|$ (dashed curve), showing that both constraints are maintained (smaller than one).

Figure 11 The impulse response of the linear-phase FIR filter.

Figure 12 The frequency response of the hearing aid, P_{ear}/P_{ext}, with the linear-phase FIR filter (solid curve) and the minimum-phase FIR filter (dashed curve).

Figure 13 The impulse response of the minimum-phase FIR filter.

Figure 14 The frequency response of the hearing aid, P_{ear}/P_{ext}, with the linear-phase FIR filters designed in the frequency domain having 309 coefficients (solid curve) and via constrained optimisation having 31 coefficients (dashed curve).

Figure 15 The magnitude response of the linear-phase FIR filter Q designed in the frequency domain (solid curve) and the linear-phase FIR filter designed via constrained optimisation (dashed curve).

Figure 16 The frequency response of the hearing aid, P_{ear}/P_{ext}, with the linear-phase FIR filter having 309 coefficients (solid curve) and the sub-band filter (dashed curve).

Figure 17 The magnitude response of the linear-phase FIR filter Q designed in the frequency domain (solid curve) and the sub-band filter (dashed curve).

Figure 18 The magnitude response of the separate sub-band filters.

Figure 19 The compensation amplification bound, as represented by $1/|WG_0|$, for various ears as measured in study [10].

Figures

Figure 1

Figure 2

Figure 3

Figure 4

Figure 5

Figure 6

28

Figure 7

Figure 8

29

Figure 9

Figure 10

Figure 11

Figure 12

Figure 13

Figure 14

32
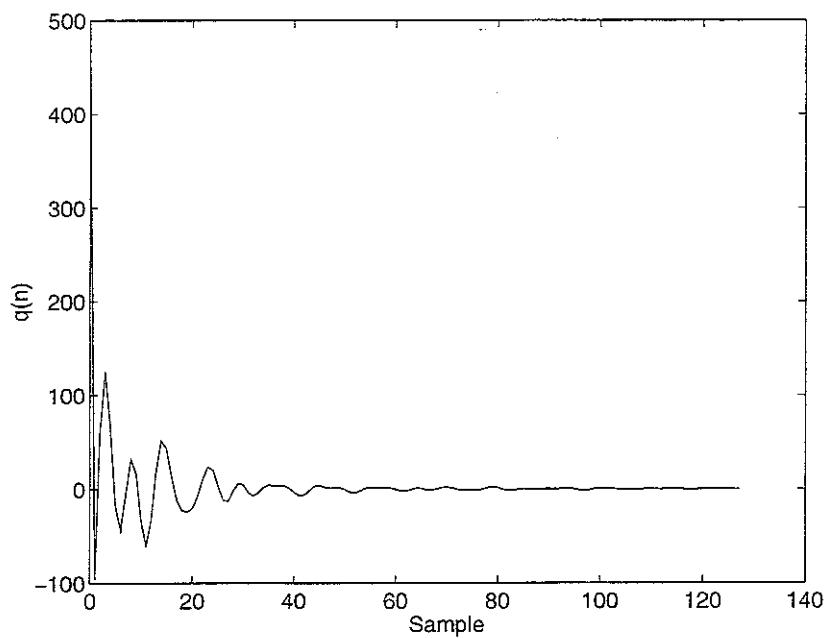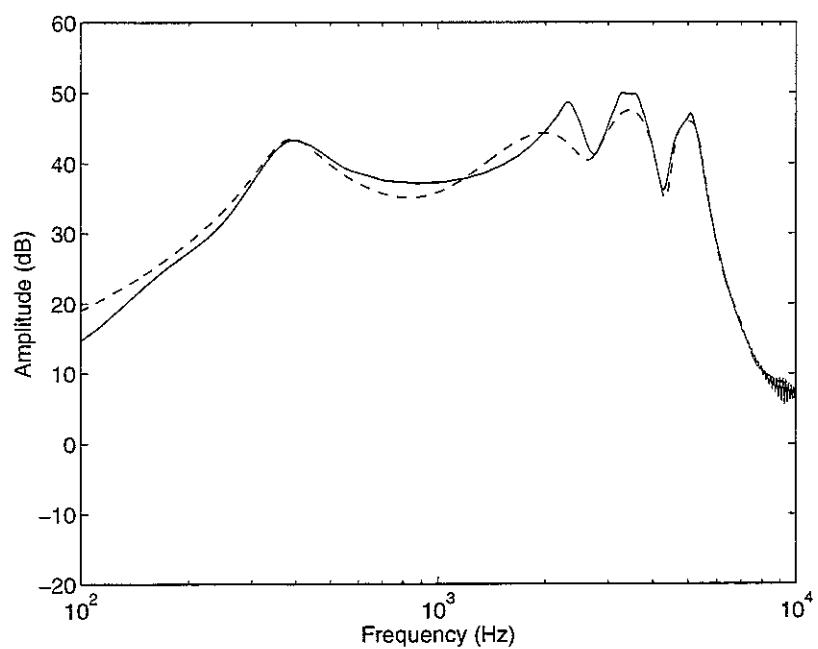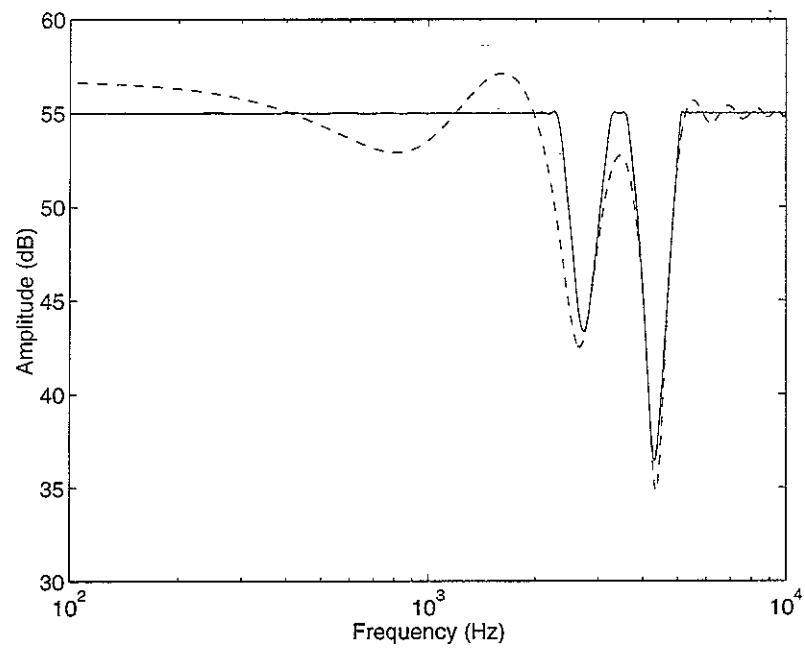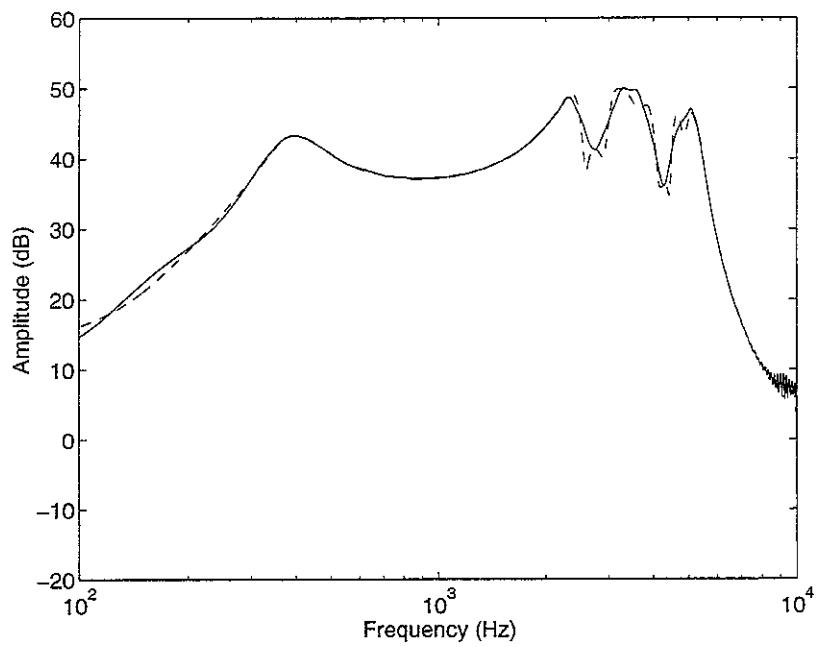
Figure 15

Figure 16

Figure 17

Figure 18

Figure 19

35